Transported Joint PDF Simulation of a Turbulent Ethanol Spray Flame Combined with a Spray Flamelet Model

Y. Hu[1], H. Olguin[1,2] and E. Gutheil[1*]
[1]Interdisciplinary Center for Scientific Computing, University of Heidelberg, Germany
[2]Department of Mechanical Engineering, Universidad Técnica Federico Santa María, Chile

1 Introduction

In spray flames, the presence of the evaporating liquid adds challenges to the modeling of these flames. Most often, in pure gas flows or flame simulations, a mixture fraction is used to describe the mixing state, and a presumed β function accounts for its turbulent character; however, this simplification is not valid in two-phase flows [1, 2]. In order to avoid this assumption, a transported probability density function (PDF) provides a suitable approach. This method also shows the advantage that the joint PDF of more than one variable about the thermo or hydro-dynamic state of flow may be included and solved without additional assumption of the statistical independence of variables, which is usually applied in the presumed PDF approach [3]. The transported PDF method was first proposed for pure gas combustion simulations [4], and it shows its great potential for a wide range of applications [3]. Some studies on the applications of this method in multiphase combustion have been reported in [5, 6].

The consideration of detailed chemistry in combustion modeling is of primary importance for a better design of efficient combustion systems. For this purpose, flamelet models provide a suitable way with reasonable computational cost [7]. Hollmann and Gutheil [8] extended this method for the generation of spray flamelet structures influenced by the evaporating fuel spray.

In the present work, a turbulent ethanol dilute spray flame is modeled using a joint mixture fraction – gas enthalpy probability density function method, where the interaction by exchange with the mean (IEM) model extended by source terms accounting for spray evaporation, is used to model the micro-mixing. Two different models for the scalar mixing time-scale including the influence of spray vaporization effects are used and discussed, where the transport equation of scalar dissipation rate is solved. Detailed chemical mechanisms and transport properties are considered through use of a spray flamelet model for turbulent spray combustion. The numerical simulation is performed for the spray flame EtF6 measured by Gounder et al. [9], where droplet size and velocity distributions as well as the gas temperature are compared and discussed.

2 Mathematical Modeling and Numerical Simulation

The numerical model includes a hybrid Reynolds Averaged Navier-Stokes (RANS) – PDF description of the continuous gas phase and a Lagrangian approach for the dispersed spray. A joint PDF describes the

Correspondence to: gutheil@iwr.uni-heidelberg.de

gas mixture fraction, ξ and the gas enthalpy, h. For these variables, the transport equation of a one-point one-time Eulerian mass density function $F(\zeta, \eta; \mathbf{x}, t)$ can be derived, and it yields

$$\begin{aligned}\frac{\partial F}{\partial t} + \frac{\partial(\widetilde{u}_i F)}{\partial x_i} - \frac{\partial}{\partial x_i}\left(\Gamma_\mathrm{t}\frac{\partial(F/\langle\rho\rangle)}{\partial x_i}\right) \\ = -\frac{\partial}{\partial\zeta}\left(\left\langle\frac{1}{\rho}\frac{\partial}{\partial x_i}\left(\Gamma_\mathrm{M}\frac{\partial\xi}{\partial x_i}\right) + \frac{1}{\rho}(1-\xi)S_\mathrm{v}\middle|\zeta,\eta\right\rangle F\right) \\ -\frac{\partial}{\partial\eta}\left(\left\langle\frac{1}{\rho}\frac{\partial}{\partial x_i}\left(\Gamma_\mathrm{h}\frac{\partial h}{\partial x_i}\right) + \frac{1}{\rho}(S_\mathrm{e} - hS_\mathrm{v})\middle|\zeta,\eta\right\rangle F\right) + \frac{\langle S_\mathrm{v}\rangle}{\langle\rho\rangle}F,\end{aligned} \tag{1}$$

where, $\widetilde{u}_i$ is mean gas velocity. ζ and η are the sample space of gas mixture fraction and gas enthalpy, respectively. S_v and S_e [8] represent the spray source terms of the mass and energy, respectively. In Eq. (1), the terms on the left hand side present the changes of the joint PDF in the physical space, and the terms on the right hand side represent the transport in sample space due to the molecular diffusion as well as the effect of spray evaporation on the PDF. Compared to the transport equation derived earlier [5], the source term accounting for spray evaporation in the continuity equation of the gas phase is included in the present derivation of Eq. (1). The terms describing the molecular diffusion depend on multipoint information, and they require modeling.

In order to solve this high-dimensional joint PDF transport equation, a Monte Carlo particle method is used [4], and in the present work, an extended interaction-by-exchange-with-the-mean (IEM) model is applied to account for molecular mixing in the two-phase flows [5]. Solution of the PDF transport equation is then transformed to numerically solving the following set of stochastic differential equations (SDEs)

$$\mathrm{d}x_i^* = \left(\widetilde{u}_i + \frac{1}{\langle\rho\rangle}\frac{\partial\Gamma_\mathrm{t}}{\partial x_i}\right)\mathrm{d}t + \left(\frac{2}{\langle\rho\rangle}\Gamma_\mathrm{t}\right)^{1/2}\mathrm{d}W_i \tag{2}$$

$$\mathrm{d}\xi^* = \left(-\frac{1}{2}\omega_\phi(\xi^* - \langle\xi\rangle) + (1-\langle\xi\rangle)\frac{\langle S_\mathrm{v}\rangle}{\langle\rho\rangle}\right)\mathrm{d}t \tag{3}$$

$$\mathrm{d}h^* = \left(-\frac{1}{2}\omega_\phi(h^* - \langle h\rangle) + \frac{1}{\langle\rho\rangle}(\langle S_\mathrm{e}\rangle - \langle h\rangle\langle S_\mathrm{v}\rangle)\right)\mathrm{d}t. \tag{4}$$

Equation (2) is needed to determine the particle position. The superscript $*$ denotes the particle properties, and these equations give the evolution of stochastic gas particle's position x_i^*, mixture fraction ξ^* and gas enthalpy h^*. Γ_t is the turbulent transport coefficient given by $\Gamma_\mathrm{t} = \mu_\mathrm{t}/\mathrm{Sc_t}$. $\mu_\mathrm{t} = C_\mu\langle\rho\rangle\widetilde{k}^2/\widetilde{\epsilon}$ the turbulent viscosity, where k and ϵ are the turbulent kinetic energy and its dissipation rate, respectively. $\mathrm{d}W_i$ is the increment of a stochastic Wiener process, which is determined from a Gaussian random number generator with mean $\langle\mathrm{d}W_i(t)\rangle = 0$ and covariance $\langle\mathrm{d}W_i(t)\mathrm{d}W_j(t)\rangle = \mathrm{d}t\delta_{ij}$. $\omega_\phi = 2\widetilde{\chi}/\widetilde{\xi^{"2}}$ is the scalar mixing frequency, and $\widetilde{\xi^{"2}}$ is the variance of the mixture fraction and $\chi = \overline{D(\partial\xi^{"}/\partial x_i)^2}$ the scalar dissipation rate, where D is the molecular diffusion coefficient.

Commonly, the modeling of $\widetilde{\chi}$ is based on an algebraic representation with the assumption that time and length scales of the scalar and the large-scale turbulence are proportional

$$\widetilde{\chi} = \frac{C_\phi}{2}\widetilde{\xi^{"2}}\omega_\mathrm{t}, \tag{5}$$

here $\omega_\mathrm{t} = \widetilde{\epsilon}/\widetilde{k}$ is the frequency of turbulent mixing. C_ϕ is a model constant with a standard value of 2. C_ϕ is not a universal parameter and the performance of the PDF model calculations would strongly depend on the mixing model and the specified value of C_ϕ [10]. Recent studies [11, 12] also show that

in the two-phase flows, the dissipation rate of a scalar presents a more complicated trend of variation, and the mixing is enhanced due to multiphase mass transfer. Direct solution of the transport equation of the scalar dissipation rate appears to be a promising way to avoid empirical parameters and to explicitly include the influence of spray evaporation. Gomet et al. [13, 14] proposed a modeled transport equation of the scalar dissipation rate for evaporating spray flows, where a linear closure of the terms for evaporation effects is adopted. In the present study, a model is derived based on a two-scale direct interaction approximation of Yoshizawa [15] with the following formulation for $\widetilde{\chi}$

$$\frac{\mathrm{D}\widetilde{\chi}}{\mathrm{D}t} = \lambda_1 \frac{\widetilde{\chi}}{\widetilde{\xi^{"2}}} \frac{\mathrm{D}\widetilde{\xi^{"2}}}{\mathrm{D}t} + \lambda_2 \frac{\widetilde{\chi}}{\widetilde{\epsilon}} \frac{\mathrm{D}\widetilde{\epsilon}}{\mathrm{D}t}, \tag{6}$$

where $\mathrm{D}/\mathrm{D}t$ denotes the material derivative. After inserting the modeled transport equations for $\widetilde{\xi^{"2}}$ and $\widetilde{\epsilon}$ with consideration of the spray source terms [5, 8] into Eq. (6), and rearrangement of terms, yields

$$\begin{aligned} \frac{\partial \langle\rho\rangle \widetilde{\chi}}{\partial t} + \frac{\partial}{\partial x_i}\left(\langle\rho\rangle \widetilde{u}_i \widetilde{\chi} - \Gamma_\chi \frac{\partial \widetilde{\chi}}{\partial x_i} \right) = & \underbrace{\alpha_P \frac{\mu_\mathrm{t}}{Sc_\mathrm{t}} \frac{\widetilde{\chi}}{\widetilde{\xi^{"2}}} \left(\frac{\partial \widetilde{\xi}}{\partial x_i} \right)^2}_{\mathrm{S1}} + \underbrace{\beta_P \frac{\widetilde{\chi}}{\widetilde{k}} \left(G_k - \frac{2}{3} \langle\rho\rangle \widetilde{k} \frac{\partial \widetilde{u}_j}{\partial x_j} \right)}_{\mathrm{S2}} \\ & \underbrace{- \alpha_D \langle\rho\rangle \frac{\widetilde{\epsilon\chi}}{\widetilde{k}}}_{\mathrm{S3}} \underbrace{- \beta_D \langle\rho\rangle \frac{\widetilde{\chi}^2}{\widetilde{\xi^{"2}}}}_{\mathrm{S4}} + \underbrace{\lambda_1 \frac{\widetilde{\chi}}{\widetilde{\xi^{"2}}} S_{\widetilde{\xi^{"2}}} + \lambda_2 \frac{\widetilde{\chi}}{\widetilde{\epsilon}} S_{\widetilde{\epsilon}} + (1 - \lambda_1 - \lambda_2) \widetilde{\chi} S_\mathrm{v}}_{\mathrm{S5}}, \end{aligned} \tag{7}$$

with

$$G_k = \mu_\mathrm{t} \left\{ \left(\frac{\partial \widetilde{u}_j}{\partial x_i} + \frac{\partial \widetilde{u}_i}{\partial x_j} \right) - \frac{2}{3} \left(\frac{\partial \widetilde{u}_k}{\partial x_k} \right) \delta_{ij} \right\} \frac{\partial \widetilde{u}_i}{\partial x_j}. \tag{8}$$

Here, the gradient diffusion approximation is used to evaluate the diffusion term of $\widetilde{\chi}$. The term S5 accounts for spray evaporation effects, and it includes the spray source terms [8] $S_{\widetilde{\xi^{"2}}}$ and $S_{\widetilde{\epsilon}}$ for mixture fraction variance $\widetilde{\xi^{"2}}$ and dissipation rate $\widetilde{\epsilon}$, respectively. The model constants are $\alpha_P = 2.0$, $\beta_P = 0.72$, $\alpha_D = 0.96$, $\beta_D = 2.0$, and $\lambda_1 = 1.0$, $\lambda_2 = 0.5$ [16]. Compared with Eq. (7), the model used by Gomet et al. [13] has a similar form with model parameters $\alpha_P = 2\omega_\mathrm{t}/\omega_\phi$, $\beta_P = 2.0$, $\alpha_D = -1.0$, and $\beta_D = 2.0$, and the evaporation effect term S5 is given by $2\widetilde{\chi}S_\mathrm{v}$. To demonstrate the performance of the models for the scalar dissipation rate, simulations with the algebraic formulation Eq. (5), transport equation, Eq. (7) and model by Gomet et al. [14] are carried out, and the computed results are compared. The different models are denoted by SD_AM, SD_TM1 and SD_TM2, respectively, in the results' section.

A spray flamelet structure is used to describe the detailed chemistry. Compared with the classical flamelet model [7], the spray flamelet model considers the effects of evaporating droplets on the laminar flamelet. These effects are included in pre-calculated counterflow spray flame structures with the consideration of detailed chemistry for ethanol/air combustion including 38 species and 337 elementary reactions [17]. In this case, additional spray parameters are taken into account, and the formulation for the mean scalars $\widetilde{\Phi}$ are given as

$$\widetilde{\Phi} = \int_0^\infty \int_{-\infty}^\infty \int_0^\infty \int_0^\infty \int_0^1 \Phi \ \widetilde{f}(\xi, \chi, R_0, v_0, E) \ \mathrm{d}\xi \ \mathrm{d}\chi \ \mathrm{d}R_0 \ \mathrm{d}v_0 \ \mathrm{d}E. \tag{9}$$

R_0 and v_0 denote the initial droplet radius and velocity, respectively, and E is the global equivalence ratio at the spray inlet.

3 Results and Discussion

EtF6 is a dilute turbulent spray flame with liquid ethanol in air. The spray burner shown in Fig. 1 is composed of a central fuel jet with nozzle diameter D = 10.5 mm, around which is a pilot jet flame with diameter 25 mm to stabilize the main flame. A coflow air stream with a velocity of 4.5 m/s is provided within a diameter of 104 mm. The profiles at the first experimental cross-section are used to generate inlet profiles [18]. More details about the experimental setup are provided by Gounder et al. [9].

Figure 2 shows the radial profiles of computed and experimental gas phase temperature at different axial locations. The comparison shows the numerical results generally follow the trend of experimental data, although at the downstream location x/D = 30, the gas temperature is overestimated. This over-prediction indicates that in this simulation, the spreading of the jet downstream is not as fast as in the experiment. As pointed out by Chrigui et al. [19], this discrepancy could partly result from errors in the experiment, where the measurement is performed using sensitive thermocouple elements. In Figs. 3 and 4, the computed Sauter mean diameter (SMD) and the axial mean and fluctuating droplet velocities are compared with the experimental data at axial locations x/D = 10 and 30. The computed SMD starts from a high value near the center line and decreases towards the edge of jet flame. Generally, good agreement with the experiment is achieved. Comparatively, the droplet axial velocities match reasonably with the experiments at upstream locations x/D = 10, and at x/D = 30, discrepancies are found, which again implies that further downstream, the turbulent intensity is underestimated.

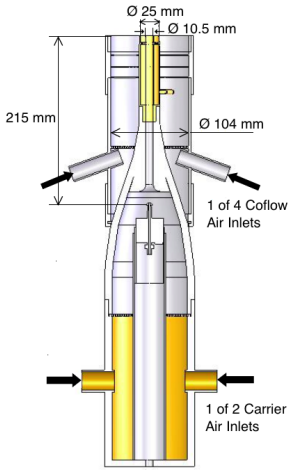

Figure 1: Geometry of the experimental configuration [9].

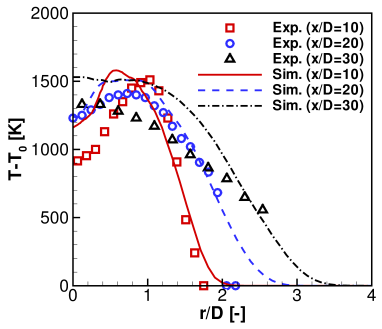

Figure 2: Radial profiles of gas excess temperature at different distances from the nozzle exit.

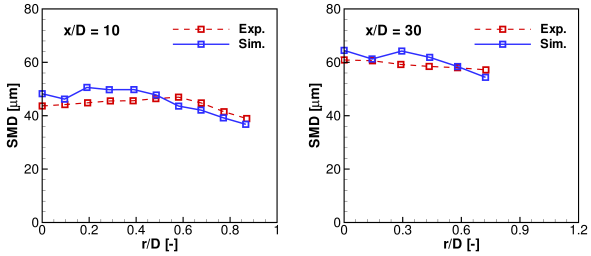

Figure 3: Radial profiles of the Sauter mean diameter, SMD at x/D = 10 and 30.

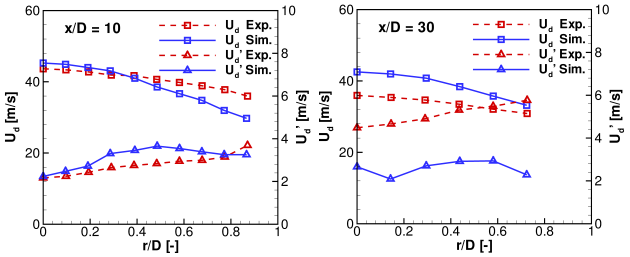

Figure 4: Radial profiles of axial mean and fluctuating droplet velocities at x/D = 10 and 30.

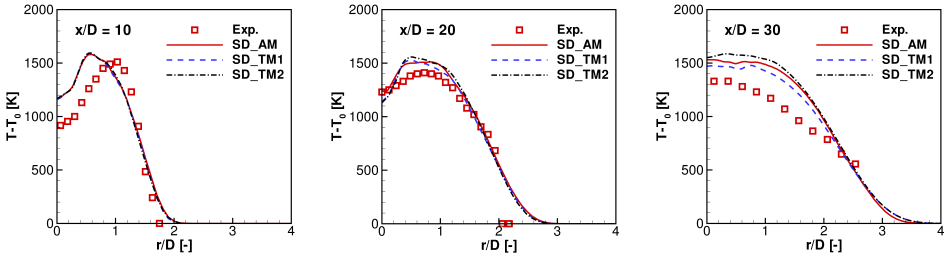

Figure 5: Comparison of radial profiles of gas phase excess temperature at x/D = 10, 20 and 30.

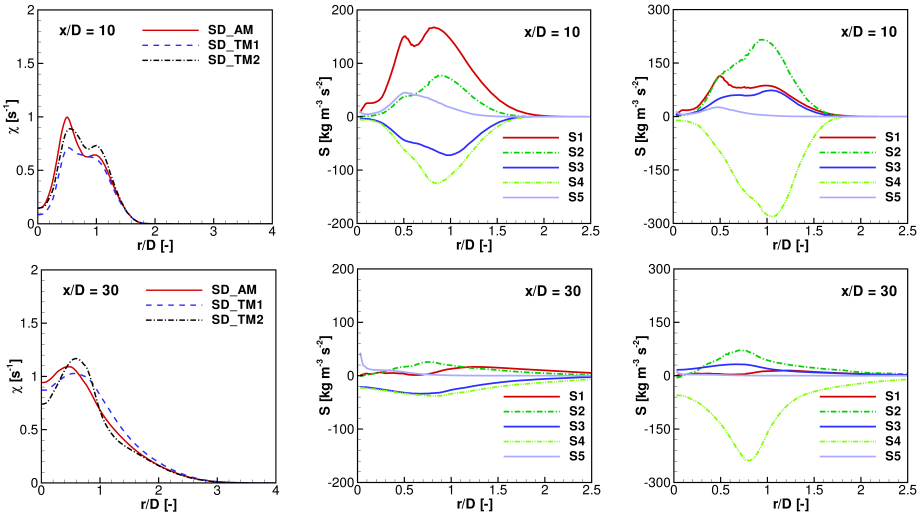

Figure 6: Radial profiles of scalar dissipation rate $\widetilde{\chi}$ (left) and right-hand side source terms of $\widetilde{\chi}$ in Eq. (7); (center: SD_TM1; right: SD_TM2) .

Figure 5 presents a comparison of the computed gas temperature using different models for $\widetilde{\chi}$ and measurements at cross-sections x/D = 10 and 30. The differences between the models upstream are small and become more obvious at higher distances from the nozzle exit, where the temperature using SD_TM1 is lower than that obtained using SD_TM2. The comparison of the computed $\widetilde{\chi}$ profiles and the analysis of right hand side source terms in the transport equation for $\widetilde{\chi}$ is shown in Fig. 6. It can be seen that using the SD_TM2 model, the production term, S2, due to mean velocity gradients is always positive and presents the dominating term, while in the SD_TM1 model, S1 the production term due to mean concentration gradients appears to be more important. The peak value of $\widetilde{\chi}$ in SD_TM1 is lower than in SD_TM2.

4 Conclusions

The numerical simulation of the EtF6 spray flame [9] is performed using a combined approach including a transported joint PDF of gas enthalpy and mixture fraction of gaseous species and a spray flamelet model for ethanol/air combustion. Different models for the scalar dissipation rate of the mixture fraction do not show significant differences, and for the present jet flame, the algebraic model of χ is suitable, cf. Eq. (5). For more complex spray flames, this conclusion may need reconsideration. All major spray flame characteristics including Sauter mean diameter, spray velocity and its turbulent fluctuation as well as gas temperature show good agreement with experimental results.

References

[1] H.-W. Ge and E. Gutheil (2006). Probability density function (PDF) simulation of turbulent spray flows. Atomiz. Sprays 16: 531.

[2] K. Luo and H. Pitsch and M. G. Pai and O. Desjardins (2011). Direct numerical simulations and analysis of three-dimensional n-heptane spray flames in a model swirl combustor. Proc. Combust. Inst. 33: 2143.

[3] D. C. Haworth (2010). Progress in probability density function methods for turbulent reacting flows. Prog. Energy Combust. Sci. 36: 168.

[4] S. B. Pope (1985). PDF methods for turbulent reactive flows. Prog. Energy Combust. Sci. 11: 119.

[5] H.-W. Ge and E. Gutheil (2008). Simulation of a turbulent spray flame using coupled PDF gas phase and spray flamelet modeling. Combust. Flame 153: 173.

[6] P. Jenny and D. Roekaerts and N. Beishuizen (2012). Modeling of turbulent dilute spray combustion. Prog. Energy Combust. Sci. 38: 846.

[7] N. Peters (2000). Turbulent combustion. Cambridge Univ. Press,Cambridge.

[8] C. Hollmann, E. Gutheil (1998). Flamelet-Modeling of Turbulent Spray Diffusion Flames Based on a Laminar Spray Flame Library. Combust. Sci. and Tech. 135: 175.

[9] J. D. Gounder and A. Kourmatzis and A. R. Masri (2012). Turbulent piloted dilute spray flames: Flow fields and droplet dynamics. Combust. Flame 159: 3372.

[10] R. R. Cao, H. Wang and S. B. Pope (2007). The effect of mixing models in PDF calculations of piloted jet flames. Proc. Combust. Inst. 31: 1543.

[11] S. Sreedhara, Kang Y. Huh (2007). Conditional statistics of nonreacting and reacting sprays in turbulent flows by direct numerical simulation. Proc. Combust. Inst. 31: 2335.

[12] J. Reveillon, F. Demoulin (2007). Effects of the preferential segregation of droplets on evaporation and turbulent mixing. J. Fluid Mech. 583: 273.

[13] L. Gomet, V. Robin and A. Mura (2012). Influence of Residence and Scalar Mixing Time Scales in Non-Premixed Combustion in Supersonic Turbulent Flows. Combust. Sci. and Tech. 184: 1471.

[14] L. Gomet, V. Robin and A. Mura (2014). Lagrangian modelling of turbulent spray combustion under liquid rocket engine conditions. Acta Astronaut. 94: 184.

[15] A. Yoshizawa (1988). Statistical modeling of passive-scalar diffusion in turbulent shear flows. J. Fluid Mech. 195: 541.

[16] J. P. H. Sanders and I. Gökalp (1998). Scalar dissipation rate modeling in variable density turbulent axisymmetric jets and diffusion flames. Phys. Fluids 10: 939.

[17] E. Gutheil (2001). Structure and extinction of laminar ethanol-air spray flames. Combust. Theory Model. 5: 1.

[18] Y. Hu and E. Gutheil (2014). Transported Joint PDF Modeling of Dilute Turbulent Spray Flows. Sept. 8-10, ILASS-Europe 2014, Bremen, Germany.

[19] M. Chrigui, J. Gounder, A. Sadiki, J. Janicka and A. R. Masri (2013). Acetone Droplet Behavior in Reacting and Non Reacting Turbulent Flow. Flow Turbul. Combust. 90: 419.